Research Article

Electromagnetic wave propagation in a parallel-plate waveguide filled with linear metamaterials

Burhan Zamir[a,*], Aqib Nisar[b], Babar Shahzad[b]

[a]*Department of Physics, Govt. M. A. O. Graduate College, Lahore 54000, Pakistan*
[b]*Department of Physics, Division of Science & Technology, University of Education, Lahore 54700, Pakistan.*

Abstract

In this article, we present an analysis of electromagnetic wave propagation in a parallel-plate waveguide filled with (a) a conventional (linear, homogeneous and isotropic) dielectric medium (b) metamaterial. In this connection, we derive the dispersion relations for the TE and TM wave modes for both cases. The dispersion characteristics of the waves are obtained by the numerical analysis of the dispersion relation by plotting it for the propagation frequency versus the wave vector for different values of the dimensions of the waveguide and the number of modes. The dispersion characteristics show propagation and non-propagation regions in the microwave frequency range. This effect can be used for different waveguide applications e.g., filters, sensors etc.

1. Introduction

In recent years, the field of metamaterials (MTMs) has garnered significant attention due to their unique electromagnetic properties that can be tailored for specific applications [1–5]. One of the most promising applications of metamaterials is in the design of waveguides for high-frequency communication systems [6–10]. Metamaterials are engineered materials with unique electromagnetic properties that are not found in natural materials. They are designed by arranging subwavelength building blocks in a specific pattern to achieve the desired properties. Metamaterials can exhibit unusual properties such as negative refraction, cloaking, and super-resolution, which have potential applications in various fields including telecommunications [11–14]. The well-known types of metamaterials are double negative (DNG) and single negative (SNG) metamaterials. Double negative metamaterials (DNG-MTMs), also known as left-handed metamaterials [15, 16], consist of a composite of two materials, one with negative permittivity and the other with negative permeability. The idea of left-handed metamaterials was developed theoretically by Veselago [16] in 1968.

Later, Pendry et al. [17–19], Smith et al. [20], and Shelby et al. [21] experimentally realized the artificial negative permittivity and permeability by constructing a composite medium in microwave frequency band based on a periodic array of interspaced conducting split-ring resonators and long continuous metallic wires. This combination results in a negative refractive index and allows light to propagate in a direction opposite to that in natural materials. Single negative metamaterials (SNG-MTMs) are categorized in two categories, the materials with negative permittivity and positive permeability are termed as the epsilon negative metamaterials (ENG-MTMS), whereas materials with positive permittivity and negative permeability are called mu-negative metamaterials (MNG-MTMs). SNG-MTMs are typically easier to fabricate than double negative metamaterials, and they have potential applications [22, 23].

Parallel-plate waveguides (PPWGs) are a common type of waveguide used in the transmission of electromagnetic waves. By filling the PPWG with a metamaterial, the propagation of the waves can be controlled and manipulated in ways not possible with conventional materials. This has opened up new possibilities for the design of waveguides with improved performance (see e.g. [22] and references therein). In recent years, some research work is reported for the high-frequency electro-

*Corresponding Author:
`burhanzamir1@gmail.com` (Burhan Zamir)

magnetic wave propagation in MTM based waveguides [6–15]. In this connection, Zamir and Ali [24] investigated the change in propagation properties of a nonlinear MTM filled PPWG by replacing the perfect-conducting plates to high- temperature superconductor parallel plates. They reported some new and different aspects of the wave propagation properties which were not present in a conventional PPWG. In this research paper, we will theoretically investigate the propagation properties of a parallel-plate waveguide filled with linear metamaterials and explore the potential applications of this technology in high-frequency communication systems.

2. Theoretical analysis

In this paper, we study the electromagnetic wave propagation in a PPWG filled with linear MTMs. A schematic representation of the proposed waveguide structure is shown in Figure (1). Consider an electromagnetic wave is propagating through a parallel-plate waveguide loaded with a DNG-MTM along z-axis with profile $e^{i(\omega t - kz)}$, as shown in Figure (1). Here, ω is the propagation frequency of the electromagnetic wave and k is the propagation constant. The parallel-plates are extended infinitely in yz-plane, whereas the separation between the plates id a.
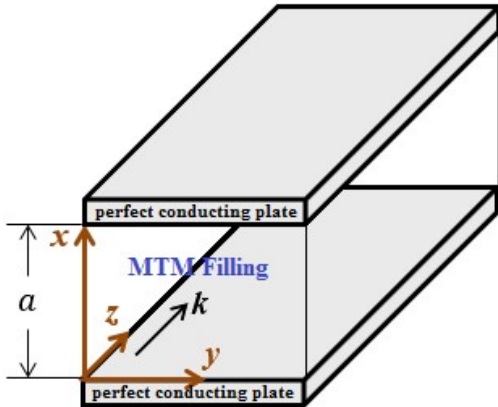

Figure 1: A PPWG filled with linear MTMs

A DNG-MTM is characterized by its simultaneously negative permittivity and permeability in a certain range of propagation frequency, given by the following relative functions:

$$\varepsilon_{DNG}(\omega) = 1 - \frac{\omega_p^2}{\omega^2} \tag{1}$$

$$\mu_{DNG}(\omega) = 1 - \frac{F\omega^2}{\omega^2 - \omega_r^2} \tag{2}$$

where ω_p is the plasma frequency, ω_r is the resonance frequency and F is the filling factor[20]. Here, without loss of generality, the damping terms are not considered [25]. The field profile for transvers electric (TE) waves have the form

$(H_x, E_y, H_z)e^{i(\omega t - kz)}$. To obtain the electromagnetic wave equation for the DNG-MTM, we first take the Maxwell field equations as

$$\nabla \times H = i\omega\varepsilon_\circ\varepsilon_{DNG}(\omega)E \tag{3}$$

$$\nabla \times E = -i\omega\mu_\circ\mu_{DNG}(\omega)H \tag{4}$$

For the case of TE wave mode, Equations (3) and (4) have been used to obtain the following wave equation for E_y:

$$\frac{d^2 E_y}{dx^2} + k_\circ^2 \varepsilon_{DNG}(\omega)E_y - k^2 E_y = 0 \tag{5}$$

where $K_\circ^2 = \frac{\omega^2}{c^2}$. The solution of the above wave equation is given by

$$E_y = c_1 \sin k_{DNG} x + c_2 \cos k_{DNG} x \tag{6}$$

Here $k_{DNG} = \left[k_\circ^2 \varepsilon_{DNG}(\omega)\mu_{DNG}(\omega) - k^2\right]^{1/2}$. c_1 and c_2 are arbitrary constants and can be evaluated from the boundary conditions. Solution in Eq. (4) is used in Equation (4) to derive the following field components for TE-mode:

$$H_x = \frac{-k}{\omega\mu_{DNG}(\omega)\mu_\circ}(c_1 \sin k_{DNG}x + c_2 \cos k_{DNG}x) \tag{7}$$

$$H_z = \frac{ik_{DNG}}{\omega\mu_{DNG}(\omega)\mu_\circ}(c_1 \cos k_{DNG}x - c_2 \sin k_{DNG}x) \tag{8}$$

A similar mathematical treatment can be performed to derive the wave equation in H_y for TM-mode to obtain the following solution:

$$H_y = c_3 \sin k_{DNG}x + c_4 \cos k_{DNG}x \tag{9}$$

where c_3 and c_4 are arbitrary constants and can be evaluated from the boundary conditions. Solution in Equation (9) is used in Equation (9) to derive the following field components for TE-mode:

$$E_x = \frac{-k}{\omega\varepsilon_\circ\varepsilon_{DNG}(\omega)}(c_3 \sin k_{DNG}x + c_4 \cos k_{DNG}x) \tag{10}$$

$$E_z = \frac{ik_{DNG}}{\omega\varepsilon_\circ\varepsilon_{DNG}(\omega)}(c_3 \cos k_{DNG}x + c_4 \sin k_{DNG}x) \tag{11}$$

2.1. The dispersion relation

To find the dispersion relation for the TE and TM waves, we employ the following boundary conditions for the continuity on the field components at $x = 0$:

$$\text{TE Waves :} \begin{cases} E_y|_{x=0} \\ E_y|_{x=d} \end{cases} \tag{12}$$

$$\text{TM Waves :} \begin{cases} H_y|_{x=0} \\ H_y|_{x=d} \end{cases} \tag{13}$$

Using the values of E_y from Eq. (6) to Eq. (12), we obtain the following dispersion relation for TE mode:

$$k^2 = k_\circ^2 \varepsilon_{DNG}(\omega)\mu_{DNG}(\omega) - n^2\pi^2/a^2 \qquad (14)$$

where $n = 1, 2, 3, \dots$, known as number of modes. Similarly, using the values of H_y from Eq. (9) to Eq. (13), we obtain the dispersion relation for TM-mode which is exactly the same as given in Eq. (14).

2.2. Case of MNG-MTM

For the case of a PPWG loaded with MNG-MTM, we consider positive value of nonlinear permittivity i.e. ε_{MNG} (not a function of frequency) and frequency dependent negative permeability $\mu_{MNG}(\omega) = 1 - \omega_{mp}^2/\omega^2$, where ω_{mp} is the magnetic plasma frequency for MNG-MTM [26–28]. Therefore Eq. (5) can be written as

$$\frac{d^2 E_y}{dx^2} + k_\circ^2 \varepsilon_{MNG}\mu_{MNG}(\omega)E_y - k^2 E_y = 0 \qquad (15)$$

and the solution of Eq. (6) becomes

$$E_y = c_5 \sin k_{MNG} x + c_6 \cos k_{MNG} x \qquad (16)$$

where $k_{MNG} = \left[k_\circ^2 \varepsilon_{MNG}\mu_{MNG}(\omega) - k^2\right]^{1/2}$. The corresponding magnetic field components for TE-mode i.e. H_x and H_z are obtained from Eq. (4) and these are given by

$$H_x = \frac{-k}{\omega\mu_{MNG}(\omega)\mu_\circ}(c_5 \sin k_{MNG} x + c_6 \cos k_{MNG} x) \qquad (17)$$

$$H_z = \frac{ik_{MNG}}{\omega\mu_{MNG}(\omega)\mu_\circ}(c_5 \cos k_{MNG} x + c_6 \sin k_{MNG} x) \qquad (18)$$

Similarly, for TM-mode, the corresponding field components are given by

$$H_y = c_7 \sin k_{MNG} x + c_8 \cos k_{MNG} x \qquad (19)$$

$$E_x = \frac{-k}{\omega\varepsilon_\circ\varepsilon_{MNG}}(c_7 \sin k_{MNG} x + c_8 \cos k_{MNG} x) \qquad (20)$$

$$E_z = \frac{ik_{MNG}}{\omega\varepsilon_\circ\varepsilon_{MNG}}(c_7 \cos k_{MNG} x + c_8 \sin k_{MNG} x) \qquad (21)$$

In this case, the following dispersion relation is obtained, for both TE and TM-modes, by applying the boundary conditions on Eq. (12) and (13) to Eqns. (16) and (19)

$$k^2 = k_\circ^2 \varepsilon_{MNG}\mu_{MNG}(\omega) - n^2\pi^2/a^2 \qquad (22)$$

2.3. Case of ENG-MTM

For the case of PPWG loaded with an ENG-MTM, we consider frequency dependent negative permittivity i.e., $\varepsilon_{ENG}(\omega) = 1 - \omega_{ep}^2/\omega^2$, and a constant positive value of permeability μ_{ENG}, where ω_{ep} is the electron plasma frequency for ENG-MTM [26–28]. Therefore, Eq. (5) can be written as

$$\frac{d^2 E_y}{dx^2} + k_\circ^2 \varepsilon_{ENG}(\omega)\mu_{ENG}E_y - k^2 E_y = 0 \qquad (23)$$

and the solution in Eq. (6) becomes

$$E_y = c_9 \sin k_{ENG} x + c_{10} \cos k_{ENG} x \qquad (24)$$

where $k_{ENG} = \left[k_\circ^2 \varepsilon_{ENG}(\omega)\mu_{ENG} - k^2\right]^{1/2}$. The corresponding magnetic field components for TE-mode i.e., H_x and H_z are obtained from Eq. (4) and these are given by

$$H_x = \frac{-k}{\omega\mu_{ENG}\mu_\circ}(c_9 \sin k_{ENG} x + c_{10} \cos k_{ENG} x) \qquad (25)$$

$$H_z = \frac{ik_{ENG}}{\omega\mu_{ENG}\mu_\circ}(c_9 \cos k_{ENG} x + c_{10} \sin k_{ENG} x) \qquad (26)$$

Similarly, for TM-mode, the corresponding field components are given by

$$H_y = c_{11} \sin k_{ENG} + c_{12} \cos k_{ENG} x \qquad (27)$$

$$E_x = \frac{-k}{\omega\varepsilon_\circ\varepsilon_{ENG}(\omega)}(c_{11} \sin k_{ENG} x + c_{12} \cos k_{ENG} x) \qquad (28)$$

$$E_z = \frac{ik_{ENG}}{\omega\varepsilon_\circ\varepsilon_{ENG}(\omega)}(c_{11} \cos k_{ENG} x + c_{12} \sin k_{ENG} x) \qquad (29)$$

In this case, the following dispersion relation is obtained, for both TE and TM-modes, by applying the boundary conditions on Eq. (12) and (13) to Eqns. (24) and (27)

$$k^2 = k_\circ^2 \varepsilon_{ENG}\mu_{ENG}(\omega) - n^2\pi^2/a^2 \qquad (30)$$

2.4. Case of conventional PPWG

For the case of PPWG loaded with a conventional dielectric material, the permittivity and permeability have constant values i.e., ε_c and μ_c. Therefore, Eq. (5) can be written as

$$\frac{d^2 E_y}{dx^2} + k_\circ^2 \varepsilon_{ENG}(\omega)\mu_{ENG}E_y - k^2 E_y = 0 \qquad (31)$$

and the solution of Eq. (6) becomes

$$E_y = c_{13} \sin k_c x + c_{14} \cos k_c x \qquad (32)$$

where $k_c = \left[k_\circ^2 \varepsilon_c\mu_c - k^2\right]^{1/2}$. The corresponding magnetic field components for TE-mode i.e. H_x and H_z are obtained from Eq. (4) and these are given by

$$H_x = \frac{-k}{\omega\mu_c\mu_\circ}(c_{13} \sin k_c x + c_{14} \cos k_c x) \qquad (33)$$

$$H_z = \frac{ik_c}{\omega\mu_c\mu_\circ}(c_{13} \cos k_c x - c_{14} \sin k_c x) \qquad (34)$$

Similarly, for TM-mode, the corresponding field components are given by

$$H_y = c_{15} \sin k_c x + c_{16} \cos k_c x \qquad (35)$$

$$E_x = \frac{-k}{\omega\varepsilon_\circ\varepsilon_c}(c_{15} \sin k_c x + c_{16} \cos k_c x) \qquad (36)$$

$$E_z = \frac{ik_c}{\omega\varepsilon_\circ\varepsilon_c}(c_{15} \cos k_c x - c_{16} \sin k_c x) \qquad (37)$$

In this case, the following dispersion relation is obtained, for both TE and TM-modes, by applying the boundary conditions in Eq. (12) and (13) to Eqns. (32) and (35)

$$k^2 = k_\circ^2 \varepsilon_c\mu_c - n^2\pi^2/a^2 \qquad (38)$$

3. Numerical Analysis

In this section, we numerically analyze the dispersion relations by plotting the propagation constant against the frequency for the wave propagation in our proposed PPWGs. In this connection, we plot and discuss the dispersion diagrams for the TE and TM waves in both (i) conventional parallel-plate waveguide and (ii) parallel-plate waveguide filled with metamaterials. Before going into the details of the dispersion diagrams, first we have to find the frequency ranges in which (i) a DNG material has simultaneously negative values of permittivity and permeability (ii) an ENG material has negative value of permittivity (iii) a MNG material has negative value of permeability.

3.1. Frequency bands for metamaterials

To find the existence frequency bands for DNG and MNG-MTMs, we plot the permittivity and permeability of each material against the propagation frequency. In this connection, consider the relative permeability and permittivity for ENG-MTM as

$$\mu_{ENG} = 1.2\,, \qquad \varepsilon_{ENG} = 1 - \frac{\omega_{ep}^2}{\omega^2} \qquad (39)$$

$$\varepsilon_{MNG} = 3\,, \qquad \varepsilon_{MNG} = 1 - \frac{\omega_{mp}^2}{\omega^2} \qquad (40)$$

where, the parameter values chosen for both ω_{ep} and ω_{mp} is 10 GHz [26]. Further, for the DNG-MTM, we plot Eq. (1) and (2) for the parameters $F = 0.56$, $\omega_r = 4 \times 10^9$ Hz and $\omega_p = 10 \times 10^9$ Hz [20, 29]. Fig. 2 shows a plot of permittivity and permeability versus the propagation frequency for a DNG-MTM. The graph shows that the frequency range in which both permittivity and permeability have simultaneously negative values extends from 4×10^9 Hz to 6×10^9 Hz, called frequency band for the existence of a DNG-MTM. Fig. 3 shows a plot of per-
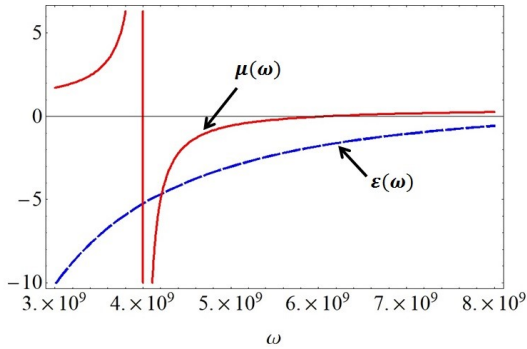
Figure 2: Plot of permittivity/permeability and frequency for a DNG-MTM

mittivity and permeability versus the propagation frequency for an ENG-MTM. The graph shows that the frequency range in which permittivity has negative value extends from 2.75×10^9 Hz to 12×10^9 Hz, called frequency band for the existence of an ENG-MTM. Fig. 4 shows a plot of permittivity and permeability versus the propagation frequency for a MNG-MTM. The graph shows that the frequency range in which permeability has

negative value extends from 3.5×10^9 Hz to 10×10^9 Hz, called frequency band for the existence of an MNG-MTM.
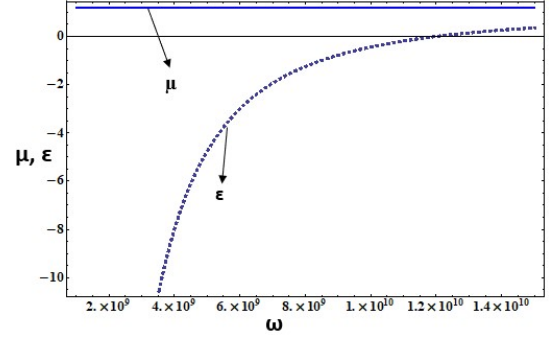
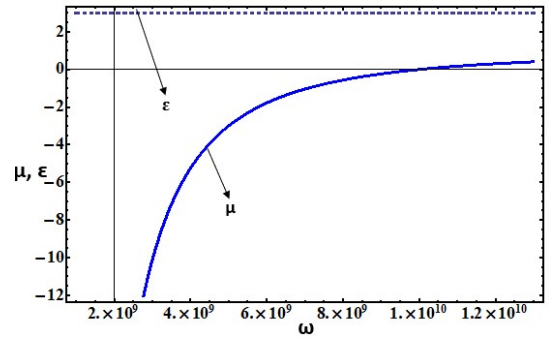Figure 3: Plot of permittivity/permeability and frequency for a ENG-MTM

Figure 4: Plot of permittivity/permeability and frequency for a DNG-MTM

3.2. Dispersion characteristics

Table (1) shows the propagation conditions for the various materials used in our proposed PPWG. Case (a) shows that the permittivity and permeability of the medium is positive and therefore defines a right-handed or double positive material. For this case, the range of frequency considered to be in the microwave range from 109 Hz to 1012 Hz. In this case, the dispersion relation is $k = \sqrt{k_\circ^2 \varepsilon_c \mu_c - n^2\pi^2/a^2}$ as given in Eq. (38). Here, k is real for $k_\circ^2 \varepsilon_c \mu_c > \left(\frac{n\pi}{a}\right)^2$ which represents the propagation of electromagnetic waves, whereas k is imaginary for $k_\circ^2 \varepsilon_r(\omega)\mu_r(\omega) < n^2\pi^2/a^2$, which represents the non-propagation of electromagnetic waves. Therefore, we can define a cut-off frequency separating the frequency band into propagation and non-propagation regions, i.e., $k_\circ^2 \varepsilon_c \mu_c = n^2\pi^2/a^2$ for $\omega = \omega_c$, $k_\circ^2 \varepsilon_c \mu_c > n^2\pi^2/a^2$ for $\omega > \omega_c$, and $k_\circ^2 \varepsilon_c \mu_c < \pi^2/a^2$ for $\omega < \omega_c$, where $\omega_c = cn\pi/a \sqrt{\varepsilon_c \mu_c}$ is the cut-off frequency.

Fig. 5 shows a plot of dispersion relation (38) for k versus ω for a fix value of waveguide dimension (i.e., $a = 3 \times 10^{-3}$ m) and for different number of modes (i.e., $n = 1, 2, 3, \ldots$). This graph shows that the propagation region of the electromagnetic waves is above a certain frequency (i.e. cut-off frequency) for each mode. The propagation characteristics are sensitive to the

Table 1: Different cases for the permittivity and permeability of the Metamaterial

Cases	Permittivity $\varepsilon_r(\omega)$	Permeability $\mu_r(\omega)$	Product $\varepsilon_r(\omega)\mu_r(\omega)$	Range	Propagation	Non-propagation
a	$\varepsilon_r(\omega) > 0$	$\mu_r(\omega) > 0$	$\varepsilon_r(\omega)\mu_r(\omega) > 0$	$10^9 - 10^{12}$	$\omega > \omega_c$	$\omega < \omega_c$
b	$\varepsilon_r(\omega) > 0$	$\mu_r(\omega) < 0$	$\varepsilon_r(\omega)\mu_r(\omega) < 0$	$3.5 \times 10^9 - 10 \times 10^9$	Never	-
c	$\varepsilon_r(\omega) < 0$	$\mu_r(\omega) > 0$	$\varepsilon_r(\omega)\mu_r(\omega) < 0$	$2.75 \times 10^9 - 12 \times 10^9$	Never	-
d	$\varepsilon_r(\omega) < 0$	$\mu_r(\omega) < 0$	$\varepsilon_r(\omega)\mu_r(\omega) > 0$	$4 \times 10^9 - 6 \times 10^9$	Never	-

number of modes. The waveguide shows propagation in the upper region of the microwave band and there is no propagation for the lower region of the microwave band. Therefore, the parallel-plate waveguide filled with a double positive material (DPS-MTM) can be used as a high-pass filter etc.
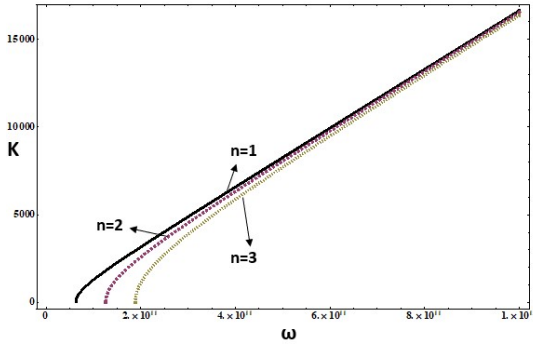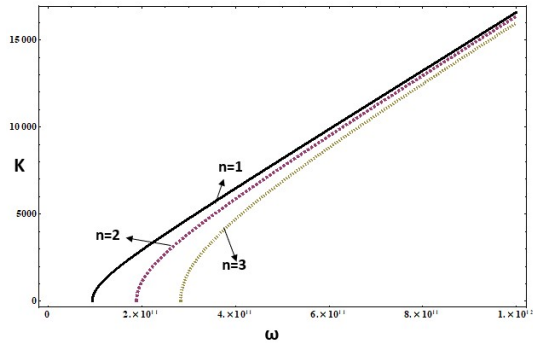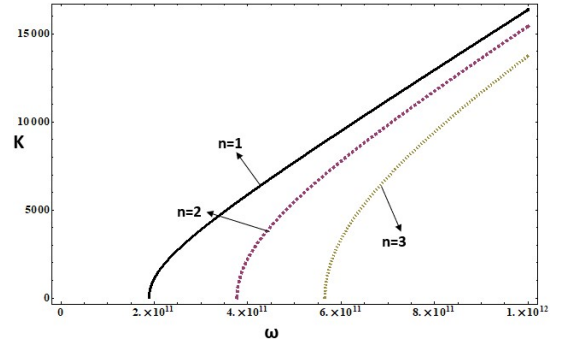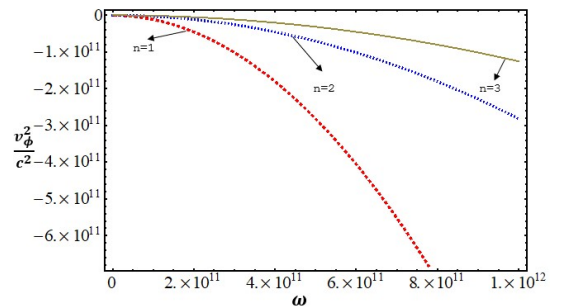

Figure 5: Dispersion diagram i.e. a plot of ω versus k for separation $a = 3 \times 10^{-3}$ m and for number of modes $n = 1, 2, 3$.

Figure 6: Dispersion diagram for separation $a = 2 \times 10^{-3}$ m and for number of modes $n = 1, 2, 3$. equation

Fig. 6 shows a plot of dispersion relation (38) for k versus ω for a fix value of plate separation (i.e., $a = 2 \times 10^{-3}$m) and for different number of modes (i.e., $n = 1, 2, 3, \ldots$). This graph shows the similar trends as discussed for Fig. 5. But here, the propagation characteristics are more sensitive to the number of modes. Further, the cut-off frequency for each mode is also different from the Fig. 5. The waveguide shows propagation in the upper region of the microwave band (i.e. from 109 Hz to 1012 Hz) and there is no propagation for the lower region of

Figure 7: Dispersion diagram for separation $a = \times 10^{-3}$ m and for number of modes $n = 1, 2, 3$.

the microwave band. Same is the case with Fig. 7, which is a plot of dispersion relation (38) for k versus ω for a fix value of plate separation (i.e., $a = 10^{-3}$ m) and for different number of modes (i.e. $n = 1, 2, 3, \ldots$). This graph shows the similar trends as discussed for Fig. 5 and 6. But here again, the propagation characteristics are more sensitive to the number of modes. Further, the cut-off frequency for each mode is also different from the Fig. 5 and 6. The waveguide shows propagation in the upper region of the microwave band (i.e. from 109 Hz to 1012 Hz) and there is no propagation for the lower region of the microwave band. Therefore, one can choose the thickness to use the parallel-plate waveguide for the particular choice of high pass filter etc.

Figure 8: Dispersion diagram of v_{φ^2}/c^2 versus ω for separation $a = 3 \times 10^{-3}$ m and for number of modes $n = 1, 2, 3$.

Case (b) and (c) show the propagation properties of the electromagnetic waves in MNG-MTM and ENG-MTM, respectively. Since, for an MNG-MTM, $\varepsilon_{MNG} > 0$ and $\mu_{MNG}(\omega) < 0$,

for which $\varepsilon_{MNG}\mu_{MNG}(\omega) < 0$, therefore, in the dispersion relation, $k = \sqrt{k_\circ^2\varepsilon_{MNG}\mu_{MNG}(\omega) - n^2\pi^2/a^2}$, k is always imaginary for this region within the frequency band of an MNG-MTM. Hence, electromagnetic waves cannot propagate in a parallel-plate waveguide filled with an MNG-MTM. Similarly, for an ENG-MTM, $\varepsilon_{ENG}(\omega) < 0$ and $\mu_{ENG} > 0$, for which $\varepsilon_{ENG}(\omega)\mu_{ENG} < 0$, so, in the dispersion relation, $k = \sqrt{k_\circ^2\varepsilon_{ENG}\mu_{ENG}(\omega) - n^2\pi^2/a^2}$, k is always imaginary for this region within the frequency band of an ENG-MTM. Hence, electromagnetic waves cannot propagate in a parallel-plate waveguide filled with an ENG-MTM.

Case (d) represents the propagation characteristics of the electromagnetic waves in DNG-MTM Since, for a DNG-MTM, $\varepsilon_{DNG}(\omega) < 0$ and $\mu_{DNG}(\omega) < 0$ for which $\varepsilon_{DNG}(\omega)\mu_{DNG}(\omega) > 0$. In dispersion relation, $k = \sqrt{k_\circ^2\varepsilon_{DNG}\mu_{DNG}(\omega) - n^2\pi^2/a^2}$, the frequency at which propagation may occur, does not exist in the existence band of a DNG-MTM (i.e., 4×10^9 Hz to 6×10^9 Hz) for the value of PPWG thicknesses $a < 10$mm. For the frequency range of simultaneous negative values of permittivity and permeability, the dispersion relation (14) does not show the region of propagation for different values of PPWG thickness a and for different values of modes n. Hence, electromagnetic waves cannot propagate in a parallel-plate waveguide filled with a DNG-MTM with the mentioned parameters. To show this finding, we present a graph of dispersion relation (14) for the normalized squared phase velocity v_φ^2/c^2 against the propagation frequency ω, within the frequency band of a DNG-MTM i.e., from 4×10^9 Hz to 6×10^9 Hz, as shown in Fig. 8. To show the non-propagation region in this graph, we write the dispersion relation (14) in the form of v_φ^2/c^2 as

$$\frac{v_\varphi^2}{c^2} = \left\{\varepsilon_{DNG}(\omega)\mu_{DNG}(\omega) - (cn\pi/\omega a)^2\right\}^{-1} \qquad (41)$$

where, v_φ^2 is the square of phase velocity and c is the speed of light in vacuum. Fig. 8 is a plot of dispersion relation (14) for normalized squared phase velocity $\frac{v_\varphi^2}{c^2}$ versus ω for a fix value of plate separation (i.e., $a = 3 \times 10^{-3}$ m) and for different number of modes (i.e., $n = 1, 2, 3, \ldots$). The graph shows that the $\frac{v_\varphi^2}{c^2} < 0$ for the whole frequency band of a DNG-MTM, therefore, electromagnetic waves cannot propagate in a parallel-plate waveguide filled with a DNG-MTM.

4. Conclusion

In this research work, we analyze the electromagnetic wave propagation in a parallel-plate waveguide filled with a (a) conventional (linear, homogeneous and isotropic) dielectric medium (b) metamaterials. In this connection, we derived the field vectors and dispersion relations for the TE and TM wave modes for both cases. The dispersion characteristics of the waves are obtained by the numerical analysis of the dispersion relation. It is seen from the graph between permittivity and permeability versus the propagation frequency that the frequency band for the existence of ENG-MTM exists between 2.75×10^9 Hz and 12×10^9 Hz .The frequency range for DNG-MTM in which

both permittivity and permeability have simultaneously negative values exists between 4×10^9 Hz and 6×10^9 Hz. Further, The frequency band for the existence of MNG-MTM is between 3.5×10^9 Hz and 10×10^9 Hz.

For a PPWG filled with a conventional dielectric medium, the dispersion curves show propagation of electromagnetic waves in upper region of microwave band but no propagation is seen in lower region within the microwave frequency range. Further, for a PPWG filled with a conventional dielectric medium, increasing the thickness between the plates of parallel-plate waveguide the propagation of electromagnetic waves also increases and vice versa. It is concluded that the propagation characteristics of electromagnetic are sensitive to the number of modes and the thickness of the waveguide. For a PPWG filled with a DNG-MTM, the frequency at which propagation may occur, does not exist in the existence band of a DNG-MTM for the value of PPWG thickness $a < 10$mm, whereas for very large plate separations, electromagnetic waves may propagate within the existence range of a DNG-MTM. Further, it is observed that electromagnetic waves cannot propagate in a parallel-plate waveguide filled with an MNG or ENG-MTM. Within the frequency bands for the existence of these MTMs, the dispersion relation does not show the region of propagation.

References

[1] N. Engheta, R. W. Ziolkowski, A positive future for double-negative metamaterials, IEEE Transactions on microwave theory and techniques 53 (4) (2005) 1535–1556.

[2] N. Engheta, R. W. Ziolkowski, Metamaterials: physics and engineering explorations, John Wiley & Sons, 2006.

[3] K. Y. Kim, Comparative analysis of guided modal properties of double-positive and double-negative metamaterial slab waveguides., Radioengineering 18 (2).

[4] M. Lapine, I. V. Shadrivov, Y. S. Kivshar, Colloquium: nonlinear metamaterials, Reviews of Modern Physics 86 (3) (2014) 1093.

[5] G. V. Eleftheriades, K. G. Balmain, Negative-refraction metamaterials: fundamental principles and applications, John Wiley & Sons, 2005.

[6] Y. Xiang, X. Dai, S. Wen, D. Fan, Properties of omnidirectional gap and defect mode of one-dimensional photonic crystal containing indefinite metamaterials with a hyperbolic dispersion, Journal of Applied Physics 102 (9) (2007) 093107.

[7] Y. Xiang, X. Dai, S. Wen, Omnidirectional gaps of one-dimensional photonic crystals containing indefinite metamaterials, JOSA B 24 (9) (2007) 2033–2039.

[8] W. Zhang, Y. Chen, P. Hou, J. Shi, Q. Wang, Transformation of nonlinear behaviors: from bright-to dark-gap soliton in a one-dimensional photonic crystal containing a nonlinear indefinite metamaterial defect, Physical Review E 82 (6) (2010) 066601.

[9] J. Yao, X. Yang, X. Yin, G. Bartal, X. Zhang, Three-dimensional nanometer-scale optical cavities of indefinite medium, Proceedings of the National Academy of Sciences 108 (28) (2011) 11327–11331.

[10] K. Kim, Y. Cho, Comparing guided modal properties of surface waves along single-and double-negative indexed slab waveguides, Opto-Electronics Review 18 (2010) 388–393.

[11] Y. Xiang, X. Dai, S. Wen, Negative and positive goos–hänchen shifts of a light beam transmitted from an indefinite medium slab, Applied Physics A 87 (2007) 285–290.

[12] Y. Xiang, X. Dai, J. Guo, H. Zhang, S. Wen, D. Tang, Critical coupling with graphene-based hyperbolic metamaterials, Scientific reports 4 (1) (2014) 5483.

[13] Y. Xiang, X. Dai, S. Wen, D. Fan, Independently tunable omnidirectional multichannel filters based on the fractal multilayers containing negative-index materials, Optics letters 33 (11) (2008) 1255–1257.

[14] Y. Xiang, J. Guo, X. Dai, S. Wen, D. Tang, Engineered surface bloch waves in graphene-based hyperbolic metamaterials, Optics Express 22 (3) (2014) 3054–3062.

[15] Y. G. Smirnov, D. V. Valovik, Guided electromagnetic waves propagating in a plane dielectric waveguide with nonlinear permittivity, Physical Review A 91 (1) (2015) 013840.

[16] V. G. Veselago, The electrodynamics of substances with simultaneously negative values of ε and μ, Soviet Physics Uspekhi 10 (4) (1968) 509.

[17] J. B. Pendry, A. Holden, W. Stewart, I. Youngs, Extremely low frequency plasmons in metallic mesostructures, Physical review letters 76 (25) (1996) 4773.

[18] J. B. Pendry, A. Holden, D. Robbins, W. Stewart, Low frequency plasmons in thin-wire structures, Journal of Physics: Condensed Matter 10 (22) (1998) 4785.

[19] J. B. Pendry, A. J. Holden, D. J. Robbins, W. Stewart, Magnetism from conductors and enhanced nonlinear phenomena, IEEE transactions on microwave theory and techniques 47 (11) (1999) 2075–2084.

[20] D. R. Smith, W. J. Padilla, D. Vier, S. C. Nemat-Nasser, S. Schultz, Composite medium with simultaneously negative permeability and permittivity, Physical review letters 84 (18) (2000) 4184.

[21] R. A. Shelby, D. R. Smith, S. Schultz, Experimental verification of a negative index of refraction, science 292 (5514) (2001) 77–79.

[22] A. Alù, N. Engheta, Guided modes in a waveguide filled with a pair of single-negative (sng), double-negative (dng), and/or double-positive (dps) layers, IEEE Transactions on Microwave Theory and Techniques 52 (1) (2004) 199–210.

[23] H. Jiang, H. Chen, H. Li, Y. Zhang, J. Zi, S. Zhu, Properties of one-dimensional photonic crystals containing single-negative materials, Phys. Rev. E 69 (2004) 066607.

[24] B. Zamir, R. Ali, Wave propagation in parallel-plate waveguides filled with nonlinear left-handed material, Chinese Physics B 20 (1) (2011) 014102.

[25] M. Shen, S. Pang, J. Zheng, J. Shi, Q. Wang, Nonlinear surface polaritons in indefinite media, JOSA B 29 (2) (2012) 197–202.

[26] S. R. Entezar, Frequency tuneable single-negative bistable heterostructure, Progress In Electromagnetics Research M 14 (2010) 33–44.

[27] W.-H. Lin, C.-J. Wu, S.-J. Chang, Angular dependence of wave reflection in a lossy single-negative bilayer, Progress In Electromagnetics Research 107 (2010) 253–267.

[28] A. Namdar, S. R. Entezar, H. Rahimi, H. Tajalli, Backward tamm states in 1d single-negtaive metamaterials photonic crystals, Progress In Electromagnetics Research Letters 13 (2010) 149–1159.

[29] I. V. Shadrivov, A. A. Sukhorukov, Y. S. Kivshar, A. A. Zharov, A. D. Boardman, P. Egan, Nonlinear surface waves in left-handed materials, Physical Review E 69 (1) (2004) 016617.